



Phenyl-substituted planar binuclear phthalocyanines: synthesis and investigation of physicochemical properties

Tatiana V. Dubinina^{a,b,*}, Stanislav A. Trashin^{b,1}, Natalia E. Borisova^a, Irina A. Boginskaya^c, Larisa G. Tomilova^{a,b,1}, Nikolay S. Zefirov^a

^a Chemistry Department, M.V. Lomonosov Moscow State University, 1 Leninskie Gory, 119991 Moscow, Russian Federation

^b Institute of Physiologically Active Compounds, Russian Academy of Sciences, 1 Severny proezd, 142432 Chernogolovka, Moscow Region, Russian Federation

^c Institute for Theoretical and Applied Electromagnetics, Russian Academy of Sciences, 125412, 13 Izhorskaya St., Moscow, Russian Federation

ARTICLE INFO

Article history:

Received 30 August 2011
Received in revised form
17 October 2011
Accepted 18 October 2011
Available online 2 November 2011

Keywords:

Naphthalocyanines
NIR absorption
Electrochemistry
Nanoparticles
Pi interactions
Binuclear phthalocyanines

ABSTRACT

Dodeca-phenyl-substituted planar binuclear phthalocyanine magnesium complexes with an extended π -conjugation system were synthesized with high yields. Two approaches to the extension of the π -system were presented: extension of an aromatic bridge or a peripheral π -system. A maximum of near-IR absorption at 972 nm was observed in the case of the planar binuclear naphthalocyanine sharing a common benzene ring. Binuclear phthalocyanines were characterized by high resolution MALDI-TOF mass spectrometry, UV/Vis/NIR and ¹H NMR spectroscopy. DFT modeling of the structure and chemical shift GIAO calculations were made. The formation of nanoaggregates in a solid film was proven using AFM. The electrochemical properties of binuclear naphthalocyanine complexes were investigated for the first time.

© 2011 Elsevier Ltd. All rights reserved.

1. Introduction

Phthalocyanines with an extended π -conjugation system are of increasing importance due to the presence of absorption in the near-IR region. This peculiarity allows for the use of planar binuclear phthalocyanines as components of photogalvanic cells [1], optical electronic devices for the near-IR region [2], photooxidative catalysis [3] and laser assisted processes [4]. The phthalocyanines possessing narrow absorption in the near-IR region have been well-studied [5–9]. However, the absorption maximum of these compounds is often too sharp and does not coincide well with the wavelengths of laser light [4]. Planar binuclear phthalocyanines have potential for this application since some electron transitions corresponding to Q-bands occupy a wide region of wavelengths in the near-IR region [4,10–13]. Moreover, the Q-band position can be controlled using the extension of the π -system.

The extension of the π -system of planar binuclear phthalocyanines can be performed in two ways: extension of an aromatic bridge or a peripheral π -system. Attempts at aromatic bridge extension from benzene to naphthalene [14–16] and tetracene [17] have been described in the literature. For these binuclear species, absorption in the near-IR region was not found. However, in our previous work, [11] it was shown that the extension of an aromatic bridge leads not to the disappearance of but to the hypsochromic shift of the Q-band.

In order to expand the peripheral π -system, an asymmetrical binuclear compound containing phthalocyanine and naphthalocyanine moieties was obtained [4,18]. Synthetic approaches to symmetrical binuclear naphthalocyanine complexes have been recently described [12,19]. The highest value of bathochromic shift of the Q-band was reached by us in the case of dodeca-substituted planar binuclear naphthalocyanine sharing a common benzene ring [19].

Because of the different substituents and central ions, which include considerable contributions to spectral properties, the literature data on planar binuclear phthalocyanines were difficult to systematize. Moreover, electrochemical investigations on planar binuclear naphthalocyanines have not been carried out.

The main purpose of this work was to determine the correlation between the extension of the aromatic system and the position of

* Corresponding author. Chemistry Department, M.V. Lomonosov Moscow State University, 1 Leninskie Gory, 119991 Moscow, Russian Federation. Fax: +7 (495) 939 0290.

E-mail addresses: dubinina.t.vid@gmail.com (T.V. Dubinina), tom@org.chem.msu.ru (L.G. Tomilova).

¹ Fax: +7 496 524 9508.

absorption in the near-IR region. Using a previously reported approach [11], a series of phenyl-substituted planar binuclear phthal- and naphthalocyanines possessing an extended π -system by an aromatic bridge or peripheral π -system were obtained. Furthermore, planar binuclear naphthalocyanine sharing a common naphthalene ring was synthesized for the first time.

2. Experimental

2.1. Chemicals and instruments

Column chromatography was carried out on neutral MN-Aluminiumoxid. Preparative TLC was performed using Merck Aluminium Oxide F₂₅₄ neutral flexible plates. Gel permeation chromatography was accomplished on the polymeric support Bio-Beads S-X1 (BIORAD). The electrolyte [Bu₄N][BF₄] (Sigma–Aldrich) was recrystallized twice from ethyl acetate/hexane (9:1 V/V) and dried under vacuum at 70 °C. *o*-Dichlorobenzene (DCB, 99%, Sigma–Aldrich, HPLC-grade) for voltammetric and spectroelectrochemical studies was used as received. All other reagents and solvents were obtained or distilled according to standard procedures. The salt Mg(OAc)₂·4H₂O was dried immediately before use in a vacuum desiccator for 10 h at 110 °C. All reactions were TLC and UV/Vis controlled until complete disappearance of the starting reagents if not additionally specified.

Electronic absorption (UV/Vis) spectra were recorded on a ThermoSpectronic Helios- α spectrophotometer using quartz cells (0.5 × 1 cm). UV/Vis/NIR measurements were made with a Hitachi U-4100 spectrophotometer in quartz cells (0.5 × 1 cm). MALDI-TOF mass spectra were taken on a VISION-2000 mass spectrometer with 2-[(2E)-3-(4-*tert*-butylphenyl)-2-methylprop-2-enylidene]-malonitrile (DCTB) as the matrix. High-resolution MALDI mass spectra were registered on a Bruker ULTRAFLEX II TOF/TOF instrument with DCTB as the matrix. ¹H and ¹³C NMR spectra were recorded on a Bruker AVANCE 400 spectrometer (400.13 MHz) at 20 °C (if not additionally specified). Chemical shifts are given in ppm relative to SiMe₄.

CHN analysis was carried out using a CHNOS Element Analyzer vario MICRO.

Electrochemical measurements were carried out using IPC-Pro (Econix, Moscow, Russia) and EmStat (Palm Instrument BV, Utrecht, the Netherlands) potentiostats. Cyclic voltammetry (CVA) and square-wave voltammetry (SWVA) were performed in a conventional three electrode cell using Pt-disk (2.0 mm in diameter) working and Pt-foil counter electrodes. A calomel reference electrode (SCE, 3 M NaCl) was connected to the solution through a salt-bridge and a Luggin capillary, whose tip was placed close to the working electrode. The junction potentials were corrected by ferrocenium⁺/ferrocene (Fc⁺/Fc) couple each time after a series of measurements. Freshly distilled dichloromethane (purium, Reachim Russia) and *o*-dichlorobenzene (DCB, 99% Sigma–Aldrich, HPLC-grade) freshly passed through an Al₂O₃ layer were used as solvents, and 0.15 mol/l solution of Bu₄NBF₄ (Sigma–Aldrich, dried under vacuum at +80 °C) in *o*-dichlorobenzene containing 2–10 × 10⁻⁴ M of sample was bubbled with argon for 20 min before measurements were taken. Blank voltammograms were recorded in the same background solution.

AFM studies were carried out by means of a Solver-P47H (NT-MDT) microscope. Tapping mode and a silicon probe with gold coating for non-contact AFM were applied to obtain images. Menzel–Glaser cover slips (18 × 18 mm) were employed as the substrate. The rounding-off radius of the probe was 10 nm.

The calculations were performed using the resources of an MVS-50K supercomputer of the Joint Supercomputer Center (JSC) (www.jssc.ru). All calculations were carried out with the PRIRODA

quantum chemistry program [20,21]. The gradient-corrected exchange–correlation Perdew, Burke and Ernzerhof (PBE) functional [22,23] was used for calculations. The efficient resolution of identity (RI) and parallel implementation of evaluating both Coulomb and exchange–correlation integrals with optimized fitting Gaussian basis sets in the PRIRODA code permits the performance of calculations of the molecular systems with a large number of basic functions [20,21]. A large integration grid (which comprises about 800,000 points over the calculated molecules) with a 5 × 10⁻⁹ accuracy parameter of the adaptively generated grid was used. This parameter is responsible for the precision of the exchange–correlation energy per atom. The 10⁻⁷ threshold on the orbital gradients at the energy calculations tag and 10⁻⁵ threshold on the molecular gradient for the geometry optimization procedure were employed. In all calculations, spin-restricted formalism was chosen. For all atoms except hydrogen, SBK effective core pseudo-potentials were used [24,25] adopted for using with the program [26]. The valence shells were described by basis sets with the following contraction schemes: [311/1] on H; [611111/411/11] on C, N, and O; and [611111111/61111] on Mg atoms. All geometries were completely optimized without any symmetry constraints. Systematic vibrational analysis was performed to confirm whether an optimized geometry corresponded to a minimum without an imaginary frequency. The starting geometries were constructed analogously to known procedures [27].

2,3,6,7-Tetracyanonaphthalene and 6,7-dibromonaphthalene-2,3-dicarbonitrile were synthesized according to the published procedure [11]. The pyromellitonitrile (Aldrich) and 4,5-dichlorophthalonitrile were used without additional purification.

2.2. Synthesis and characterization

2.2.1. Preparation of 1,2-dicyano-4,5-diphenylbenzene 2

A mixture of **1** (2.00 g, 0.01 mmol), phenylboronic acid (4.36 g, 0.04 mmol), NaBr (1.06 g, 0.01 mmol) and a saturated aqueous solution of K₂CO₃ (5.6 g, 0.04 mmol) were stirred in 70 mL of boiling 1,4-dioxane under argon. The dichloro-*bis*-(triphenylphosphine) palladium compound (0.12 g, 0.0002 mmol) was added after boiling the solvent. The reaction was carried out for 6 h (TLC-control: Al₂O₃, ethyl acetate:hexane (1:10)). The reaction mixture was cooled to room temperature and water was added. The product was collected by extraction with ethyl acetate. The residue was treated by flash chromatography (ethyl acetate:hexane (1:10)) to give pale yellow crystals of **2** (2.59 g, 92%). The target compound was additionally purified by sublimation. *R*_f = 0.46 (Al₂O₃, F₂₅₄, ethyl acetate:hexane (1:10)). ¹H NMR (CDCl₃): δ 7.08–7.10, 7.25–7.33 (m, 10H, H_{Ph}); 7.84 (s, 2H, H_{Ar} – 3, 6). ¹³C NMR (CDCl₃): δ 114.38 (C₁, C₂); 115.37 (CN); 128.54 (p-C_{Ph}); 128.61 (m-C_{Ph}); 129.30 (o-C_{Ph}); 135.53 (C₃, C₆); 137.61 (C₄, C₅); 145.86 (C_{Ph}-quarternary). Anal. Calc. for C₂₄H₁₄N₂: C 85.69; H 4.31; N 9.99%. Found: C 85.75, 85.63; H 4.35, 4.31; N 9.96, 10.03%.

2.2.2. Preparation of 6,7-diphenyl-naphthalene-2,3-dicarbonitrile 7

2.2.2.1. Pd(0) catalysis. A mixture of **6** (1.00 g, 3.00 mmol), phenylboronic acid (0.88 g, 7.20 mmol) and saturated aqueous solution of K₂CO₃ (5 mL) were stirred in 55 mL of boiling mixture 1,4-dioxane:acetonitrile (8:3 V/V) under argon. The *tetrakis*-(triphenylphosphine) palladium compound (0.18 g, 0.16 mmol) was added after boiling the solvent. The reaction was carried out for 6 h (TLC-control: Al₂O₃, C₆H₆). The reaction mixture was cooled to room temperature and water was added. The product was collected by extraction with ethyl acetate. The residue was treated by flash chromatography (ethyl acetate:hexane (1:2)) in order to remove the catalyst destruction products. The reaction product was additionally purified by chromatography on a column with Al₂O₃ using

a mixture of ethyl acetate:hexane (1:2) as the eluent to give pale yellow crystals of **7** (0.61 g, 61%), m.p. 230–230.3 °C, $R_f = 0.73$ (Al_2O_3 , F_{254} , ethyl acetate:hexane (1:2)). ^1H NMR (CDCl_3): δ 7.15–7.21 (m, 4H, o- H_{Ph}); 7.25–7.33 (m, 6H, p- H_{Ph} , m- H_{Ph}); 7.99 (s, 2H, $\text{H}_{\text{Ar}} - 5, 8$); 8.37 (s, $\text{H}_{\text{Ar}} - 1, 4$). ^{13}C NMR (CDCl_3): δ 110.19 (s, C2, C3); 115.99 (s, CN); 127.79 (s, p- C_{Ph}); 128.31 (s, o- C_{Ph}); 129.71 (s, m- C_{Ph}); 129.96 (s, C5, C8), 132.41 (s, C6, C7), 135.69 (s, C1, C4), 139.47 (s, C9, C10), 144.46 (s, C_{Ph} -quaternary). MS (EI) m/z : 330 (M^+). Anal. Calc. for $\text{C}_{24}\text{H}_{14}\text{N}_2$: C 87.25; H 4.27; N 8.48%. Found: C 87.27, 86.92; H 4.33, 4.33; N 8.77, 8.68%.

2.2.2.2. Pd(II) catalysis. A mixture of **6** (1.80 g, 5.36 mmol), phenylboronic acid (2.28 g, 18.70 mmol) and a saturated aqueous solution of K_2CO_3 (5 mL) were stirred in 96 mL of boiling mixture 1,4-dioxane:acetonitrile (8:3 V/V) under argon. The dichloro-bis(triphenylphosphine) palladium compound (0.038 g, 0.054 mmol) was added after boiling the solvent. The reaction was carried out for 6 h (TLC-control: Al_2O_3 , C_6H_6). The reaction mixture was cooled to room temperature and water was added. The product was collected by extraction with ethyl acetate. The residue was treated by flash chromatography (ethyl acetate:hexane (1:2)) in order to remove the catalyst destruction products. The resulting compound was additionally purified by chromatography on a column with Al_2O_3 using a mixture of ethyl acetate:hexane (1:2) as the eluent to give pale yellow crystals of **7** (1.5 g, 85%).

The characteristics were identical with those obtained by method (a).

2.2.3. Preparation of (bis(7²,8²,12²,13²,17²,18²-hexaphenyltribenzo [g,l,q]-5,10,15,20-tetraazaporphyrino)-[b,e]benzene) dimagnesium **4a**

A mixture of **3a** (17.0 mg, 0.08 mmol), **2** (449.0 mg, 1.60 mmol) and $\text{Mg}(\text{OAc})_2 \cdot 4\text{H}_2\text{O}$ (69.0 mg 0.32 mmol) in *i*-AmOH (10 mL) in the presence of DBU (0.5 mL) was heated to reflux under argon for 19 h. The reaction mixture was cooled to room temperature and a mixture of $\text{MeOH}:\text{H}_2\text{O}$ (5:1 V/V) was added. The precipitate was filtered and washed with water and MeOH. The target compound was separated using gel permeation chromatography (C_6H_6 :Py (50:1 V/V)). The solvent was evaporated, and the resulting oil was washed with *n*-hexane. The precipitate was filtered off and repeatedly washed with *n*-hexane and methanol to give **4a** (26.0 mg, 17.0%). MS (MALDI-TOF), m/z : 1908 [$\text{M}]^+$. UV–VIS [THF, $\lambda_{\text{max}}/\text{nm}$ (I/I_{max}): 372(1), 698(0.56), 846(0.66)]. ^1H NMR (THF- d_8) δ : 7.17–7.19, 7.23–7.24 (m, 60H, H_{Ph}); 7.85 (s, 12H, H_{Per}); 10.72 (s, 2H, H_{Ar}).

The 2,3,9,10,16,17,23,24-octa-phenyl-phthalocyanine magnesium **5** (100.0 mg) was separated using gel permeation chromatography. MS (MALDI-TOF), m/z : 1146 [$\text{M}]^+$. UV–VIS [THF, $\lambda_{\text{max}}/\text{nm}$ (I/I_{max}): 364 (0.43), 622 (0.16), 658 (0.14), 688 (1.00)]. ^1H NMR (THF- d_8) δ : 7.21–7.45 (m, 40H, H_{Ph}); 8.66 (s, 8H, H_{Per}).

2.2.4. Preparation of (bis(9²,10²,14²,15²,19²,20²-hexaphenyltribenzo [g,l,q]-7,12,17,22-tetraazaporphyrino)-[b,g]naphthalene) dimagnesium **4b**

A mixture of **3b** (17.0 mg, 0.065 mmol), **2** (363.0 mg, 1.30 mmol) and $\text{Mg}(\text{OAc})_2 \cdot 4\text{H}_2\text{O}$ (56.0 mg, 0.26 mmol) in *i*-AmOH (5 mL) in the presence of DBU (0.5 mL) was heated to reflux under argon for 7 h. The reaction mixture was cooled to room temperature and a mixture $\text{MeOH}:\text{H}_2\text{O}$ (5:1 V/V) was added. The precipitate was filtered and washed with water and MeOH. The target compound **4b** (25.0 mg, 19%) was separated using gel permeation chromatography (C_6H_6 :Py (50:1 V/V)). The asymmetrical substituted monophthalocyanine magnesium complex (39.0 mg) and monophthalocyanine **5** (87.0 mg) were separated using gel permeation chromatography (THF). MS (MALDI-TOF), m/z : 1958 [$\text{M}]^+$. UV–VIS

[THF, $\lambda_{\text{max}}/\text{nm}$ (I/I_{max}): 368(1), 716(0.86), 798(0.29)]. ^1H NMR (DMF- d_7) δ : 7.28–7.45 (m, 60H, H_{Ph}); 7.64 (s, 12H, H_{Per}); 9.47 (s, 4H, H_{Ar}).

The characteristics of asymmetrical substituted monophthalocyanine magnesium complex **4c**: MS (MALDI-TOF), m/z : 1112 [$\text{M} + \text{H}]^+$, 1094 [$\text{M}-\text{NH}_3$] $^+$, 1067 [$\text{M}-\text{NH}_3-\text{CN}$] $^+$, 1041 [$\text{M}-\text{NH}_3-2\text{CN}$] $^+$. UV–VIS [THF, $\lambda_{\text{max}}/\text{nm}$ (I/I_{max}): 369(0.77), 647(0.19), 722(1.00), 816(0.06).

2.2.5. Preparation of (bis(8²,9²,15²,16²,22²,23²-hexaphenyltrinaphthalo [h,o,v]-5,12,19,26-tetraazaporphyrino)-[b,e]benzene) dimagnesium **8a**

A mixture of **3a** (13.0 mg, 0.06 mmol), **7** (400.0 mg (1.21 mmol)) and $\text{Mg}(\text{OAc})_2 \cdot 4\text{H}_2\text{O}$ (51.4 mg, 0.24 mmol) in *i*-AmOH (15 mL) in the presence of DBU (0.5 mL) was heated to reflux under argon for 12 h. The reaction mixture was cooled to room temperature and a mixture $\text{MeOH}:\text{H}_2\text{O}$ (5:1 V/V) was added. The precipitate was filtered and washed with water and MeOH. The target compound **8a** was separated using gel permeation chromatography (THF). The solvent was evaporated, and the resulting oil was washed with *n*-hexane. The precipitate was filtered off and repeatedly washed with *n*-hexane and methanol to give **8a** (41.0 mg, 31%). MS (MALDI-TOF), m/z : 2285 [$\text{M} - \text{H} + \text{Ph}]^+$, 2209 [$\text{M}]^+$, 2133 [$\text{M} + \text{H} - \text{Ph}]^+$. UV–VIS [THF, $\lambda_{\text{max}}/\text{nm}$ (I/I_{max}): 327(1), 772(0.33), 960(0.17)]. ^1H NMR (THF- d_8) δ : 7.23–7.24 (m, 60H, H_{Ph}); 8.20 (s, 12H, 1- H_{NPh}); 8.42 (s, 12H, 2- H_{NPh}); 9.68 (s, 2H, H_{Ar}).

The 3,4,12,13,21,22,30,31 – octa-phenyl-2,3-naphthalocyanine magnesium **9** (52.0 mg) was separated using gel permeation chromatography. MS (MALDI-TOF), m/z : 1345 [$\text{M}]^+$, 1268 [$\text{M}-\text{Ph}]^+$. UV–VIS [THF, $\lambda_{\text{max}}/\text{nm}$ (I/I_{max}): 340 (0.57), 689 (0.23), 734 (0.20), 772 (1.00)]. ^1H NMR (Py- d_5) δ : 7.26–7.31 (m, 40H, H_{Ph}); 8.13 (s, 8H, 1- H_{NPh}); 8.58 (s, 8H, 2- H_{NPh}).

2.2.6. Preparation of (bis(10²,11²,17²,18²,24²,25²-hexaphenyltrinaphthalo [j,q,x]-7,14,21,28-tetraazaporphyrino)-[b,g]naphthalene) dimagnesium **8b**

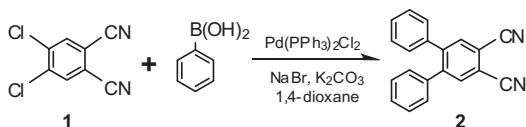
A mixture of isoindolo[5,6-*f*]isoindole-1,3,6,8(2H,7H)-tetraimine **3b** (12.0 mg, 0.046 mmol), 6,7-diphenyl-naphthalene-2,3-dicarbonitrile **7** (303.0 mg, 0.92 mmol) and $\text{Mg}(\text{OAc})_2 \cdot 4\text{H}_2\text{O}$ (39.4 mg, 0.18 mmol), in *i*-AmOH (10 mL) in the presence of DBU (0.5 mL) was heated to reflux under argon for 13 h. The reaction mixture was cooled to room temperature and a mixture $\text{MeOH}:\text{H}_2\text{O}$ (5:1 V/V) was added. The precipitate was filtered and washed with water and MeOH. The target compound **8b** was separated using gel permeation chromatography (THF). The solvent was evaporated, and the resulting oil was washed with *n*-hexane. The precipitate was filtered off and repeatedly washed with *n*-hexane and methanol to give **8b** (21.0 mg, 21%). MS (MALDI-TOF), m/z : 2259 [$\text{M}]^+$. UV–VIS [Py, $\lambda_{\text{max}}/\text{nm}$ (I/I_{max}): 331(1), 785(0.65) 916(0.14)]. ^1H NMR (Py- d_5 , 80 °C): δ 7.36–7.41 (m, 60H, H_{Ph}), 7.69 (br, 24H, H_{NPh}), 8.58 (br.s 4H, H_{Ar}).

The 3,4,12,13,21,22,30,31-octa-phenyl-2,3-naphthalocyanine magnesium **9** (269.0 mg) was separated using gel permeation chromatography.

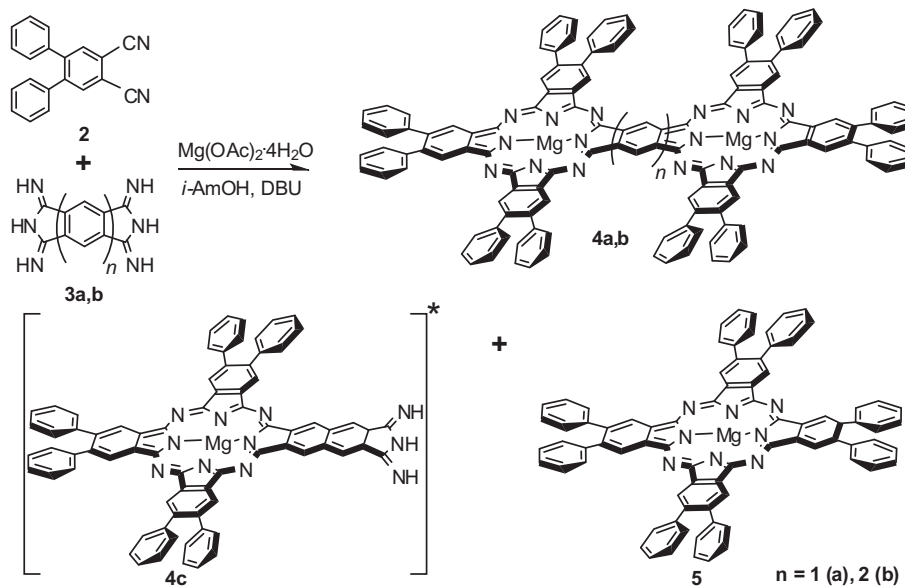
3. Results and discussion

3.1. Synthesis of binuclear phthalocyanines

Planar binuclear phthalocyanine complexes were synthesized using the statistical condensation reaction. Pyromellitonitrile and 2,3,6,7-tetracyanonaphthalene were chosen as the starting compounds for obtaining benzene and naphthalene bridges, respectively. These tetranitriles were converted to bis(diiminoisoindoline) derivatives in order to increase the reactivity in



Scheme 1. Synthesis of dinitrile **2**.



Scheme 2. Synthesis of planar binuclear phthalocyanine magnesium complexes. (*) Compound **4c** was isolated in the synthesis of **4b**.

phthalocyanine synthesis by the analogue using a published procedure [11,27].

1,2-Dicyano-4,5-diphenylbenzene was chosen as the second component of cyclization for the following reasons. First, in our previous article [11], a bathochromic shift of the Q-band for dodeca-alkyl-substituted planar binuclear phthalocyanines in comparison with hexa-alkyl-substituted ones was found. This phenomenon can be explained by the greater donor effect of twelve butyl groups than that of six *tert*-butyl groups. Second, the absence of an isomer mixture for the target phthalocyanines facilitates the interpretation of NMR spectra.

Using Suzuki–Miyaura cross-coupling (Scheme 1), 1,2-dicyano-4,5-diphenylbenzene was synthesized on the basis of 4,5-dichlorophthalonitrile **1** by the analogue using a published method [28]. Due to the in situ substitution of chlorine to bromine, the addition of NaBr provides an increasing of yield of the target compound in comparison with yields of nitriles, which were obtained by the literature procedure [28]. This approach, through the cross-coupling reaction, is most preferable for **2**, because the common procedure [29], based on the Diels–Alder reaction between diphenylacetylene and pyridazine-4,5-dicarbonitrile, led to a low yield of target compounds.

Planar binuclear phthalocyanine magnesium complexes were obtained in boiling isoamyl alcohol under argon with the addition of DBU as a base (Scheme 2). Using an excess of nitrile **2** relative to bis(diiminoisoindoline) derivative **3**, the yields of target complexes can be noticeably increased [10a,11].

Binuclear complexes **4a** and **4b** were isolated using gel permeation chromatography. Octa-phenyl-substituted monophthalocyanine **5** was the by-product of the statistical condensation reaction. Besides this, in the synthesis of **4b**, the asymmetrical substituted A₃B-type monophthalocyanine **4c** with diiminoisoindoline group was isolated and characterized by UV/Vis spectroscopy and MALDI-TOF mass spectrometry.

3.2. Synthesis of binuclear naphthalocyanines

When using 6,7-diphenyl-2,3-dicyanonaphthalene **7** as a starting compound, planar binuclear naphthalocyanine complexes were synthesized. The nitrile **7** was obtained by Suzuki–Miyaura cross-coupling on the basis of 6,7-dibromonaphthalene-2,3-

dicarbonitrile (Scheme 3). Compared with the Pd(0) catalyst, the use of the Pd(II) catalyst allowed the yield of the target compound to be increased. Perhaps this phenomenon refers to the presence of two catalytic centres in the molecule of the catalyst.

Planar binuclear naphthalocyanine magnesium complexes **8a** and **8b** were synthesized by the analogue with the synthetic procedure for the planar binuclear phthalocyanine complexes **4a** and **4b** (Scheme 4). Gel permeation chromatography was used to separate the mixture of products. The formation of only one by-product (octa-phenyl substituted monophthalocyanine magnesium complex) led to increased yields of binuclear naphthalocyanine complexes in comparison with binuclear phthalocyanine complexes.

Novel binuclear phthalo- and naphthalocyanine complexes **4** and **8** were characterized by MALDI-TOF mass spectrometry, UV/Vis/NIR and ¹H NMR spectroscopy.

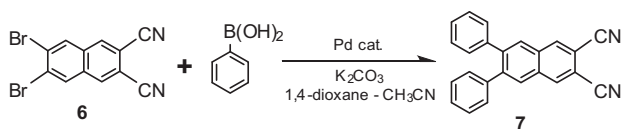
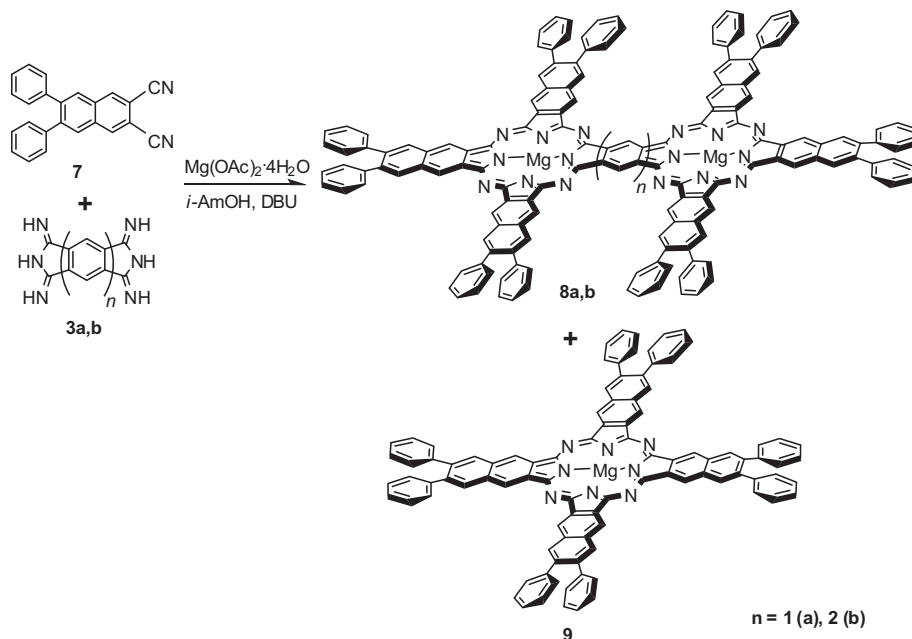
The MALDI-TOF mass spectra of these compounds (Fig. 1, DCTB² used as the matrix, and Table S1 in the Supporting Information) revealed intense molecular ion [M]⁺ peaks with characteristic isotopic patterns in good accordance with simulated ones.

It is also noteworthy that in the case of **8a**, two additional fragmentation peaks with molecular weight [M + Ph]⁺ and [M – Ph]⁺ which were formed during laser ionization were observed. The displacement of the matrix from DCTB to 9-nitroanthracene did not occur due to the disappearance of [M + Ph]⁺. So, we concluded that formation of [M + Ph]⁺ occurs after the addition of the Ph group, which was the fragment of the other binuclear molecule.

3.3. Electronic absorption spectra

In the UV/Vis/NIR spectra of binuclear phthalo- and naphthalocyanine magnesium complexes, there are two peculiarities

² DCTB – 2-[(2E)-3-(4-*tert*-butylphenyl)-2-methylprop-2-enylidene]-malonitrile.

Scheme 3. Synthesis of dinitrile **7**.

Scheme 4. Synthesis of planar binuclear naphthalocyanine magnesium complexes.

referring to the Q-band region: Q₁(blue shifted) and Q₂(red shifted). This fact could be interpreted by the split of the frontier orbitals, which has been previously calculated [12,27].

The hypsochromic shift of Q₂-band and the decrease in the Q₁–Q₂ distance going from benzene to naphthalene ring was observed (Table 1). These results correlate with LUMO destabilization for binuclear phthalocyanines sharing a common naphthalene ring in comparison with those sharing a common benzene ring [27, 30].

The extension of the peripheral π -system from binuclear phthalocyanine to naphthalocyanines resulted in a bathochromic shift of

the Q₁ and Q₂ bands, which was larger than hypsochromic shift induced by the extension of aromatic bridge. So, the Q₂-band of planar binuclear naphthalocyanine sharing a common benzene ring **8a** was the most red-shifted up to 972 nm.

It was found for the first time that in the case of binuclear phthalocyanines and naphthalocyanines with the same aromatic bridge,

the “100 nm” rule takes place: about 100 nm bathochromic shifts are observed going from **4a** to **8a** and from **4b** to **8b** (Table 1). This regularity was earlier noticed for monophthalocyanines [31] and sandwich-type [32] phthalocyanines. According to this rule, a bathochromic shift of the Q-band for naphthalocyanine **9** in comparison with phthalocyanine **5** was also observed.

The extension of the π -conjugation system for planar binuclear phthalocyanines and naphthalocyanines leads to strong π – π stacking intermolecular interactions [11]. This phenomenon results in the influence of the solvent to the character of the absorption bands (Fig. 2A).

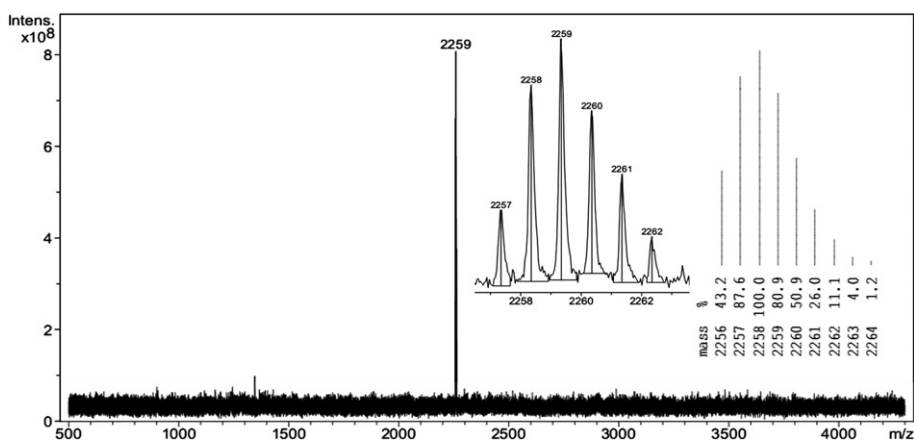


Fig. 1. MALDI-TOF mass spectrum of **8b**, isotopic patterns for the molecular ion (inset A) and simulated MS patterns of the molecular ion (inset B).

Table 1
UV/Vis/NIR of planar binuclear complexes.

Compound	λ (I/I_{\max}), nm in pyridine	λ (I/I_{\max}), nm in THF
4a	858(0.70), 696(0.57), 374(1)	846(0.66), 700(0.56), 372(1)
4b	817(0.30), 725(0.89), 371(1)	798(0.29), 716(0.86), 368(1)
5	698(1.00), 668(0.17), 628(0.19), 369(0.54)	688(1.00), 658(0.14), 622(0.16), 364(0.43)
8a	972(0.10), 786(0.37), 744(0.48), 342(1)	960(0.17), 772(0.33), 327(1)
8b	916(0.14), 785(0.65), 331(1)	905(0.18), 776(0.34), 331(1)
9	783(1.00), 744(0.15), 697(0.17), 349(0.44)	772(1.00), 733(0.15), 689(0.16), 361(0.34)

In Fig. 2A, the UV/Vis/NIR spectra of **4a** in different solvents were shown. In non-coordinating solvents (e.g. C_6H_6), a noticeable broadening of the Q-bands and B-band and a reduction in Q_2 -band intensity is observed. Similar effect was observed in the case of binuclear naphthalocyanine complexes (Fig. 3). In comparison with binuclear phthalocyanine complexes, the largest extension of the π -conjugation system for planar binuclear naphthalocyanine complexes resulted in strong aggregation effects, even in coordinating solvents. This phenomenon led to the low intensity of the Q_2 -band compared to the Q_1 -band and broadening of the absorption bands.

The UV/Vis/NIR spectrum of a **4a** thin film which was deposited from a THF solution onto a cover slip is shown in Fig. 2B. The broadening of all absorption bands, especially in the case of Q_2 , was more distinct than for non-coordinating solvents. This effect could be explained by the formation of band-type structures with strong intermolecular interactions [33]. According to the Ref [34], part of the material forms H-aggregates, which leads to hypsochromic shifted broadening of the Q-band. Another part forms J-aggregates which results in bathochromic shifted broadening of the Q-band.

3.4. 1H NMR spectroscopy of planar binuclear complexes

1H NMR study of planar binuclear phthalocyanines is associated with difficulties due to the strong aggregation at concentrations above 10^{-4} mol/l [4,14]. Broadening of signals in the aromatic area is observed and the width of signals reaches 3.7 ppm [4].

In the present study, in order to reach more distinct resolution of signals in the 1H NMR spectra, polar coordinating solvents were used (e.g. THF- d_8 , Py- d_5 and DMF- d_7). Besides this, 1H NMR spectra were recorded under high temperature to destroy aggregates.

The following regularities were found. Additional shielding of aromatic bridge protons H_{Ar} was found (Table 2), going from common benzene to the naphthalene ring by the analogue with

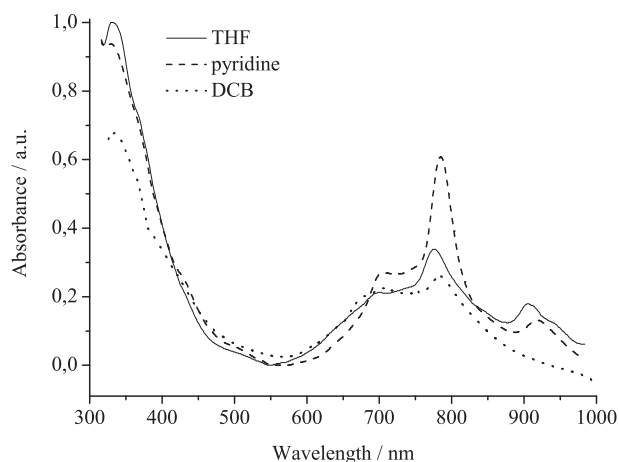


Fig. 3. UV/Vis/NIR of planar binuclear naphthalocyanine **8b**.

one, which was observed going from pyromellitonitrile (9.95 ppm) [27] to 2,3,6,7-tetracyanonaphthalene (9.01 ppm) [11]. This depends on the aromatic ring current which decreased with an increase in ring size.

For binuclear complexes **4a** and **8a** in contrast to **4b** and **8b**, the down-field shift of H_{Per} protons was found. This in turn further suggests that the ring current can be explained by a five-orbital model, taking the central TAP core and the surrounding four aromatic moieties into account, rather than a single-orbital model considering a whole molecule as a single loop [35]. The strongest aggregation effect was observed for binuclear naphthalocyanine **8b**, possessing an extended π -system by an aromatic bridge and a peripheral π -system. An equimolar amount of ethylene glycol was added to decrease the aggregation by coordination of extra ligands to the metal ion [11]. The nature of the solvent had a strong influence on the chemical shifts of phthalocyanine metal complexes, not only by their specific solvation effects, but also by the chemical interactions of the solvent with the metal ion in the phthalocyanine cavity. Such interactions could lead to significant differences between experimental and calculated chemical shift values [36] and, on the other hand, lead to strong dependencies of the chemical shifts on the nature of the solvent. Due to the low solubility of the phthalocyanine systems under the investigation, we performed NMR experiments in a wide range of polar solvents. Only two compounds, **4a** and **8a**, had enough solubility in one solvent, THF- d_8 , to make the NMR spectra comparable to each other. The spectra clearly show the great contribution of the nature

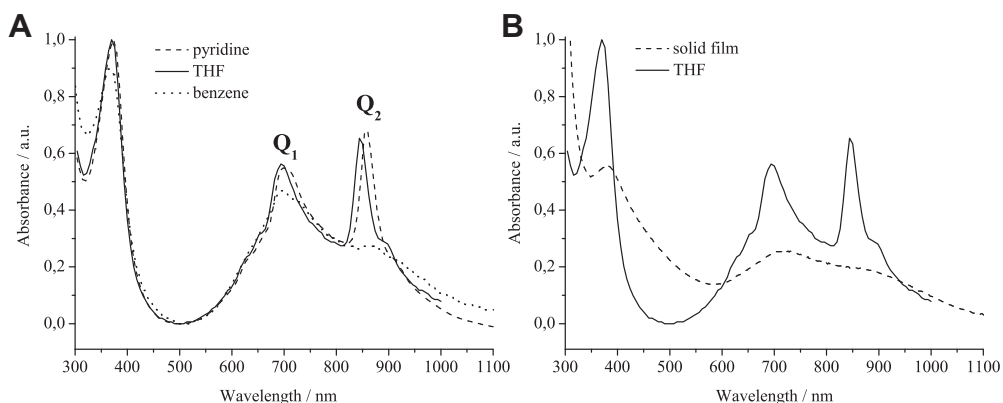


Fig. 2. UV/Vis/NIR of planar binuclear phthalocyanine **4a**.

Table 2
¹H NMR data for planar binuclear complexes.

Compound	H _{Ar}	H _{Per}	H _{Ph}	Solvent
4a	10.72 (s)	7.85 (s)	7.17–7.19, 7.23–7.24 (m)	THF-d ₈
4a^a	12.0	10.2	7.5–8.7 H _{Ph-o}	–
		9.9	7.5–8.3 H _{Ph-m}	
4b	9.47 (s)	7.64 (br.s)	7.28–7.45 (m)	DMF-d ₇
4b^a	11.1	10.1	7.4–8.5 H _{Ph-o}	–
		9.9	7.4–7.9 H _{Ph-m}	
			7.6 H _{Ph-p}	
8a	9.68 (s)	8.20 (s), 8.42 (s)	7.23–7.24 (br.m)	THF-d ₈
8a^{[19] a}	12.1	10.5 2-H _{Nph}	7.5–8.5 H _{Ph-o}	–
		10.5 2-H _{Nph}	7.6–8.1 H _{Ph-m}	
		10.8 2-H _{Nph}	7.8 H _{Ph-p}	
		9.1 1-H _{Nph}		
		9.3 1-H _{Nph}		
		9.1 1-H _{Nph}		
8b	8.58 (br.s)	7.69 (br)	7.36–7.41 (m)	Py-d ₅
8b^a	11.1	10.3 2-H _{Nph}	7.3–8.2 H _{Ph-o}	–
		10.5 2-H _{Nph}	7.4–8.0 H _{Ph-m}	
		10.3 2-H _{Nph}	7.6 H _{Ph-p}	
		8.9 1-H _{Nph}		
		9.1 1-H _{Nph}		
		9.0 1-H _{Nph}		

^a DFT calculations.

of the phthalocyanine moiety to the shifts of not only the peripheral aromatic rings of the phthal- or naphthalocyanine macrocycle but also to the shared aromatic ring. The H_{Ar} protons of the phthalocyanine **4a** are 1 ppm less shielded than that for naphthalocyanine **8a**. Contrary to the deshielding of H_{Ar}, the H_{Per} protons are 1 ppm shielded for phthalocyanine **4a**. The protons of the phenyl substituents are less affected by the expansion of the aromatic system. To elucidate the ¹H NMR spectra of the most aggregated naphthalocyanine **8b**, we performed DFT modeling of the structure of the phthalocyanines under study as well as their chemical shifts.

3.5. DFT modeling of the binuclear naphthalocyanines

DFT optimizations were made for structures **4** and **8** using the PBE functional and TZV basis set [19]. All of the structures were found to possess almost flat phthalocyanine moieties, contrary to the further investigated phenyl-substituted deformed phthalocyanines [37]. The optimized geometries are represented in the Supporting Information. The calculations of chemical shifts were made using the gauge-independent atomic orbital (GIAO) method. The calculated chemical shifts are in good agreement with the experimental data, but keep in mind that the spectra were recorded in different solvents. Strong solvent dependence was found for magnesium porphyrates [36], for which the ¹H NMR spectra were

observed in THF-d₈ and further chemical shifts were compared with GIAO calculated shifts. The calculated chemical shifts support the assignments of all of the protons; moreover, the calculations agreed with the relative shielding of the aromatic protons (H_{Ar}) and protons of peripheral rings (H_{Per}) for naphthalene-bridged molecules contrary to benzene-bridged ones. The strongest effect on the chemical shift of protons of the aromatic bridge (H_{Ar}) factor is the number of shared aromatic rings: the naphthalene-bridged molecules possess 1 ppm more shielded protons than benzene-bridged ones. This is in coincidence with the general behavior of phthalocyanines, which show a diminished ring current with the expansion of the phthalocyanine macrocycle. The number of shared aromatic rings also had an effect on the chemical shifts of the peripheral aromatics of binuclear phthalocyanine which are the most sensitive to changes from a phthalocyanine to a naphthalocyanine system. As we expected, the chemical shift of the phenyl-substituents were affected mostly by the naphthalo- or phthalocyanine macrocycle.

3.6. AFM study of thin films

An investigation of the particles which were obtained during the formation of the thin film on the cover slip was provided using AFM for binuclear complex **4a**. The concentration of the solution for deposition was about 10⁻⁶ M.

During deposition from a methanol suspension, which was preliminary held in an ultrasonic bath, the obtained films possessed an “island-type” [38], large-grain structure. The size of the grains was 4 nm in height and 250 nm in width (Fig. 4).

When depositing from a THF solution, the size of aggregates became smaller and reached 2 nm in height and 50 nm in width (Fig. 5). This fact can be explained by the coordination of solvent molecules to the magnesium ion and blocking of the formation large-scale particles by steric factors.

Thus, on the basis of AFM experiments, we showed that in the solid film the nanoparticles were formed and the size of these ones depends on the nature of the solvent.

3.7. Electrochemistry

The redox properties of the phthal- and naphthalocyanines were studied using cyclic voltammetry (CVA) and square-wave voltammetry (SWVA). Fig. 6 represents the SWVA voltammograms of phthalocyanine complexes **4a**, **b** and **5**. The voltammograms of **8a**, **b** and **9** were similar and provided in the Supporting Information.

The redox potentials and the difference of potentials between first reduction and oxidation ($\Delta E_{Ox1-Red1}$) for all studied complexes

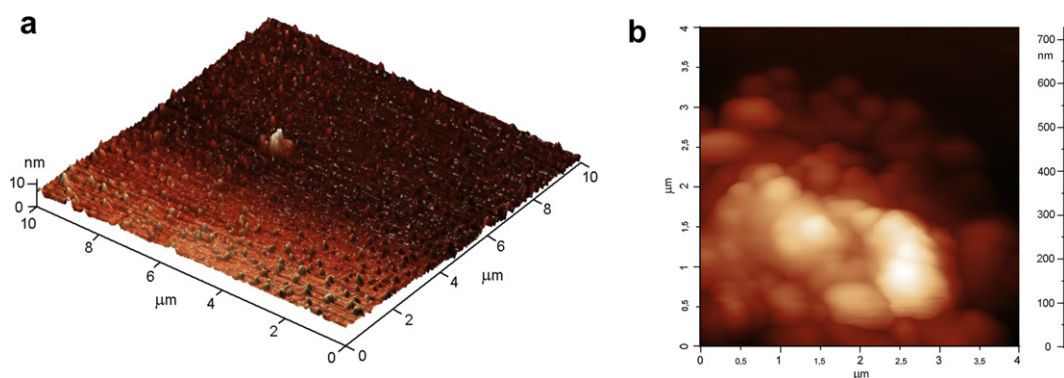


Fig. 4. AFM image of **4a** thin film a (full image) and b (fragment). (For interpretation of color referred in this figure legend the reader is referred to web version of the article.)

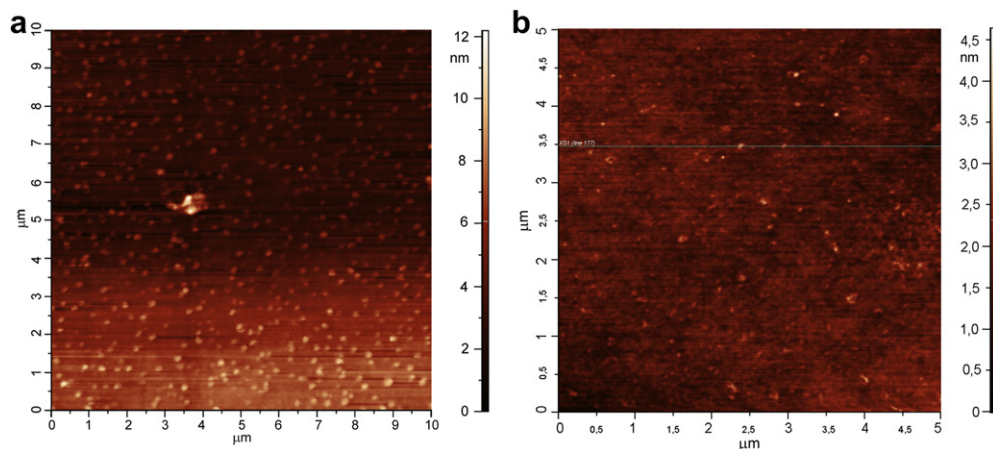


Fig. 5. AFM image of **4a** thin film deposited from a methanol suspension (a) and from a THF solution (b). (For interpretation of color referred in this figure legend the reader is referred to web version of the article.)

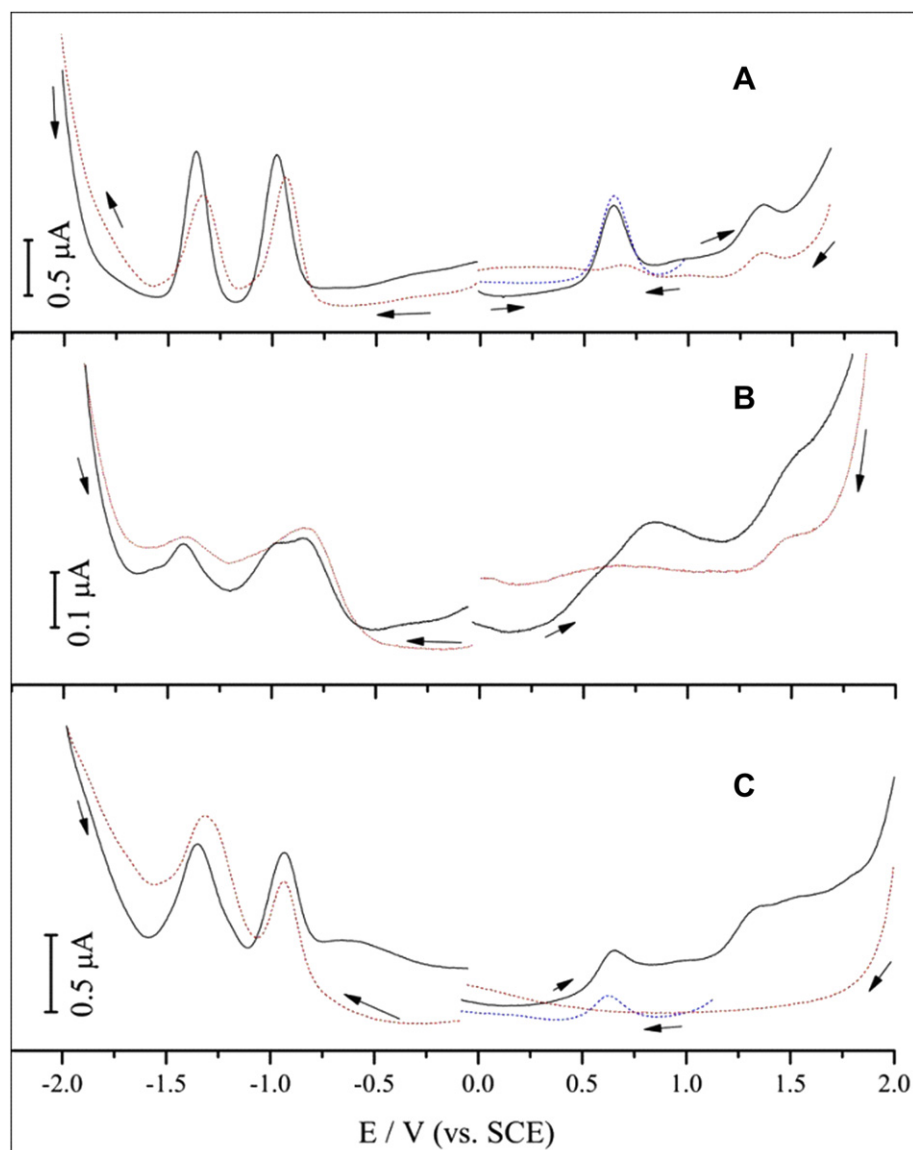


Fig. 6. SWVA of phthalocyanine complexes **5** (A), **4a** (B) and **4b** (C). Cathodic currents are shown by red dashed line, arrows gave the scan directions. The blue dashed line in (A) and (C) shows the scanning in the restricted interval. (For interpretation of color referred in this figure legend the reader is referred to web version of the article.)

Table 3
Half-wave potentials in *o*-DCB.

	Reduction			Oxidation		
	Red ₃	Red ₂	Red ₁	Ox ₁	Ox ₂	Ox ₃
5	–	–1.310	–0.926	0.636	1.258	–
4a	–	–1.426	–0.961, –0.841	–	–	1.483
4b	–	–1.332	–0.934	0.637	1.362, 1.559	1.807
9	–1.718	–1.394	–1.028	0.304	1.044	1.524
8a	–1.754	–1.477, –1.258	–1.043, –0.885	–	–	1.539
8b	–1.797	–1.396	–1.163, –1.011	0.46, 0.838	1.116, 1.316	1.541

$E_{1/2}(\text{FeFc}_2) = 0.592 \text{ V}$.

are listed in Table 3. The decrease in $\Delta E_{\text{Ox1-Red1}}$ from 1.562 V for phthalocyanine **5** to 1.332 V for naphthalocyanine **9** is in accordance with the bathochromic shift of the corresponding Q-band which is due to straight correlation between $\Delta E_{\text{Ox1-Red1}}$ and the HOMO–LUMO gap.

Unfortunately, CVAs for the binuclear complexes were not well resolved (data not shown), probably because of strong aggregation of the complexes and some irreversibility of the redox processes. However, SWVA was sensitive enough to reveal the positions of the redox processes.

Binuclear **4a**, **8a** and **8b** gave the split of Red₁ with $\Delta E_{\text{split}} = 0.15 \text{ V}$. The redox process Red₂ was split only for **8a** ($\Delta E_{\text{split}} = 0.15 \text{ V}$) but not for **8b** or **4a,b**. The benzene bridge and naphthalene periphery probably resulted in a stronger interaction between the two subunits of the binuclear complexes compared to the naphthalene bridge and benzene periphery. This is also supported by the split values of Q-bands for the complexes (Table 1). The maximal split of the Q-band was demonstrated for **8a**, while **4b** gave the minimal split.

SWVA scans in the oxidation direction showed only slightly detectable redox processes in the cases of **4a** and **8a**, and difficulties in back reduction were observed for **4b** and **8b**. Kinetic restrictions for the redox process Ox₁ were also mentioned earlier [11] for binuclear phthalocyanines with the naphthalene bridge, but spectroelectrochemistry showed that the complex can be oxidized and recovered back from the oxidized state without any losses. Absence of the oxidation processes in voltammetry for **4a** and **8a** is not well understood. However, because of the known poor reversibility of Ox₁, we could suggest that the neutral forms of the complexes **4a** and **8a** are partially oxidized into positively charged radicals or they have formed side products (e.g. with oxygen). Further spectroelectrochemical and EPR studies to clarify this behavior were performed and will be published as a separate article.

4. Conclusions

In conclusion, the approach to the synthesis of novel phenyl-substituted planar binuclear phthalocyanines and naphthalocyanines magnesium complexes has been described. For the first time, a planar binuclear naphthalocyanine sharing a common naphthalene bridge and possessing an extended π -system by an aromatic bridge and a peripheral π -system was synthesized. For all complexes, the absorption maximum was about 200 nm red-shifted in comparison with their mono-analogues. The Q₂-band of planar binuclear naphthalocyanine sharing a common benzene ring was the most red-shifted up to 972 nm. Distinct determination of redox properties for phthalocyanines and naphthalocyanines were made using SWVA. The splitting of reduction peaks was found in the case of binuclear complexes. The ¹H NMR of the compounds showed a strong dependence of the chemical shifts of the protons of the phthalocyanine-rings on the dimension of the system. The larger naphthalo-bridged and naphthalocyanine systems possessed less

desielded protons due a diminished aromatic ring current. DFT modeling of the structure and the chemical shifts of the molecules also support this observation. The calculated chemical shifts support the assignments of all of the protons; moreover, the calculations agreed with the relative shielding of the aromatic protons (H_{Ar}) and the protons of the peripheral rings (H_{Per}) for naphthalene-bridged molecules contrary to benzene-bridged ones. Using the AFM technique, we showed that in the solid film an “island-type”, large-grain structure, composed of nanoaggregates, was formed. The size of these particles depends on the nature of the solvent.

Acknowledgement

The research was supported by the Russian Foundation for Basic Research (Grant No. 08-03-00753), Sinosteel Anshan Research Institute of Thermo-Energy (RDTE) and the program of the Presidium of the Russian Academy of Science “Development of a strategy of organic synthesis and creation of compounds with valuable and applied proprieties”. We thank Institute of Biomedical Chemistry of Russian Academy of Medical Sciences for high-resolution MALDI mass spectra and Joint Supercomputer Center (JSC) for computing time on MVS-50K.

Appendix. Supplementary information

Supplementary data associated with this article can be found in the online version at doi:10.1016/j.dyepig.2011.10.012.

References

- [1] Shen Y, Zheng F, Cheng W, Gu F, Zhang J, Xia Y. Polymer photovoltaic cells by using manganese phthalocyanine derivative. *Semicond Sci Technol* 2010;25: 065016.
- [2] Feng Y, Zhang X, Feng W. Near-infrared optical response of a naphthalocyanine/few-walled carbon nanotube hybrid. *Org Electronics* 2010;11: 1016–9.
- [3] Ikeue T, Sonoda M, Kurahashi S, Tachibana H, Teraoka D, Sugimori T, et al. Annulated dinuclear palladium(II) phthalocyanine complex as an effective photo-oxidation catalyst for near-infrared region light. *Inorg Chem Commun* 2010;13:1170–2.
- [4] Kobayashi N, Higashi Y, Osa T. A planar phthalocyaninyl-naphthalocyanine as a broad near-infrared absorber. *Chem Lett*; 1994:1813–6.
- [5] Ye H, Chang Q, Wu Y, He Ch, Zuo X, Zhou J, et al. Optical limiting of metallic naphthalocyanine compound. *Mater Lett* 2003;57:3302–4.
- [6] Poon KW, Liu W, Chan PK, Yang Q, Chan TWD, Mak TCW, et al. Tetrapyrrole derivatives substituted with ferrocenylethynyl moieties. synthesis and electrochemical studies. *J Org Chem* 2001;66:1553–9.
- [7] Dubinina TV, Piskovoi RA, Tolbin AY, Pushkarev VE, Vagin MY, Tomilova LG, et al. Synthesis of new lanthanide naphthalocyanine complexes based on 6,7-bis(phenoxy)-2,3-naphthalodinitrile and their spectral and electrochemical investigation. *Izv Akad Nauk Ser Khim* 2008;57:1879–85 (*Russ Chem Bull* 2008; 57: 1912–9).
- [8] (a) Shukun Y, Chunyu M, Chuanhui C, Xu W, Dongmei J, Zhaoqi F. Synthesis and 0.88 μm near-infrared electroluminescence properties of a soluble chloroindium phthalocyanine. *Dyes Pigm* 2008;76:492–8; (b) Fukuda T, Ishiguro T, Kobayashi N. Non-planar phthalocyanines with Q-bands beyond 800 nm. *Tetrahedron Lett* 2005;46:2907–9.
- [9] Mack J, Kobayashi N. Low symmetry phthalocyanines and their analogues. *Chem Rev* 2011;111:281–321.
- [10] (a) Makarov S, Litwinski C, Ermilov EA, Suvorova O, Roder B, Wöhrle D. Synthesis and photophysical properties of annulated dinuclear and trinuclear phthalocyanines. *Chem Eur J* 2006;12:1468–74; (b) Makarov SG, Piskunov AV, Suvorova ON, Schnurpfeil G, Domrachev GA, Wöhrle D. Near-infrared absorbing ligand-oxidized dinuclear phthalocyanines. *Chem Eur J* 2007;13:3227–33; (c) Litwinski C, Corral I, Ermilov EA, Tannert S, Fix D, Makarov S, et al. Annulated dinuclear metal-free and Zn(II) phthalocyanines: photophysical studies and quantum mechanical calculations. *J Phys Chem B* 2008;112: 8466–76.
- [11] Dubinina TV, Ivanov AV, Borisova NE, Trashin SA, Gurskiy SI, Tomilova LG, et al. Synthesis and investigation of spectral and electrochemical properties of alkyl-substituted planar binuclear phthalocyanine complexes sharing a common naphthalene ring. *Inorg Chim Acta* 2010;363:1869–78.

- [12] Makarov SG, Suvorova ON, Schnurpfeil G, Wöhrle D. Synthesis of a dinuclear naphthalocyanine analogue with absorption in the NIR. *Eur J Inorg Chem*; 2010;4617–21.
- [13] Tolbin AY, Pushkarev VE, Tomilova LG, Zefirov NS. Synthesis and spectral properties of new planar binuclear phthalocyanines sharing the benzene ring. *Izv Akad Nauk Ser Khim* 2006;55:1112–5 (Russ Chem Bull 2006; 55: 1155–8).
- [14] Yang J, Mark MRVD. Synthesis of binuclear phthalocyanines sharing a benzene or naphthalene ring. *Tetrahedron Lett* 1993;34:5223–6.
- [15] Calvete M, Hanack M. A binuclear phthalocyanine containing two different metals. *Eur J Org Chem*; 2003:2080–3.
- [16] (a) Calvete MJF, Dini D, Flom SR, Hanack M, Pong RGS, Shirk JS. Synthesis of a bisphthalocyanine and its nonlinear optical properties. *Eur J Org Chem*; 2005:3499–509; (b) Calvete MJF, Dini D, Hanack M, Sancho-García JC, Chen W, Ji W. Synthesis, DFT calculations, linear and nonlinear optical properties of binuclear phthalocyanine gallium chloride. *J Mol Model* 2006;12:543–50.
- [17] Youssef TE, Hanack M. Synthesis and characterization of unsymmetrically substituted dienophilic nickel phthalocyanines for Diels–Alder reactions. *J Porphyr Phthalocyan* 2002;6:571–7.
- [18] Kobayashi N, Ogata H. Some properties and molecular orbitals of planar heterodinuclear phthalocyanines. *Eur J Inorg Chem*; 2004:906–14.
- [19] Dubinina TV, Borisova NE, Paramonova KV, Tomilova LG. Synthesis and spectral properties of dodecaphenyl-substituted planar binuclear naphthalocyanine magnesium complex sharing a common benzene ring. *Mendeleev Commun* 2011;21:165–7.
- [20] Laikov D, Ustynyuk Y. PRIRODA-04: a quantum chemical program suite. New possibilities in the study of molecular systems with the application of parallel computing. *Izv Akad Nauk Ser Khim* 2005;54:804–10 (Russ Chem Bull 2005; 54: 820–6).
- [21] Laikov DN. Fast evaluation of density functional exchange-correlation terms using the expansion of the electron density in auxiliary basis sets. *Chem Phys Lett* 1997;281:151–6.
- [22] Perdew JP, Burke K, Ernzerhof M. Generalized gradient approximation made simple. *Phys Rev Lett* 1996;77:3865–8.
- [23] Perdew JP, Burke K, Ernzerhof M. Generalized gradient approximation made simple [Phys Rev Lett 1996;77:3865], *Phys Rev Lett* 78, 1997, 1396.
- [24] Stevens WJ, Basch H, Krauss M. Compact effective potentials and efficient shared-exponent basis-sets for the 1st-row and 2nd-row atoms. *J Chem Phys* 1984;81:6026–33.
- [25] Stevens WJ, Krauss M, Basch H, Jasien PG. Relativistic compact effective potentials and efficient, shared-exponent basis sets for the third-, fourth-, and fifth-row atoms. *Can J Chem* 1992;70:612–30.
- [26] Laikov DN. A new class of atomic basis functions for accurate electronic structure calculations of molecules. *Chem Phys Lett* 2005;416:116–20.
- [27] Kobayashi N, Lam H, Nevin WA, Janda P, Leznoff CC, Koyama T, et al. Synthesis, spectroscopy, electrochemistry, spectroelectrochemistry, Langmuir–Blodgett film formation, and molecular orbital calculations of planar binuclear phthalocyanines. *J Am Chem Soc* 1994;116:879–90.
- [28] Eu S, Katoh T, Umeyama T, Matano Y, Imahori H. Synthesis of sterically hindered phthalocyanines and their applications to dye-sensitized solar cells. *Dalton Trans*; 2008:5476–83.
- [29] Turchi S, Nesi R, Giomi D. Reactions of 4,5-dicyanopyridazine with alkynes and enamines: a new straightforward complementary route to 4-mono- and 4,5-disubstituted phthalonitriles. *Tetrahedron* 1998;54:1809–16.
- [30] Kobayashi N, Konami H. Molecular orbitals and electronic spectra of phthalocyanine analogues. In: Leznoff CC, Lever ABP, editors. *Phthalocyanines: properties and applications*, vol. 4. VCH Publishers, Inc.; 1996. p. 385–7.
- [31] Lukyanets EA, Nemykin VN. The key role of peripheral substituents in the chemistry of phthalocyanines and their analogs. *J Porphyr Phthalocyan* 2010; 14:2–40.
- [32] Gal'pern MG, Talismanova TD, Tomilova LG, Luk'yanets EA. Phthalocyanines and related compounds. XXV. Tetra-5-bromo-tetra-7-tert-butyl-1-2,3-naphthalocyanines. *Zh Obshch Khim* 1985;55:1099–106 [J Gen Chem USSR 1985; 55: 980-985 (Engl. Transl.)].
- [33] Dodsworth ES, Lever ABP, Seymour P, Leznoff CC. Intramolecular coupling in metal-free binuclear phthalocyanines. *J Phys Chem* 1985;89:5698–705.
- [34] Nyokong T. Electronic spectral and electrochemical behavior of near infrared absorbing metallophthalocyanines. In: Mingos DMP, Jiang J, editors. *Electronic spectral and electrochemical behavior of near infrared absorbing metallophthalocyanines*, vol. 135. Berlin Heidelberg: Springer-Verlag; 2010. p. 62–3.
- [35] Kobayashi N, Nakajima S, Ogata H, Fukuda T. Synthesis, Spectroscopy, and electrochemistry of tetra-tert-butylated tetraazaporphyrins, phthalocyanines, naphthalocyanines, and anthracocyanines, together with molecular orbital calculations. *Chem Eur J* 2004;10:6294–312.
- [36] Kozłowski PM, Wolinski K, Pulay P, Ye BH, Li XY. GIAO nuclear magnetic shielding tensors in free base porphyrin and in magnesium and zinc metalloporphyrins. *J Phys Chem A* 1999;103:420–5.
- [37] Fukuda T, Homma S, Kobayashi N. Deformed phthalocyanines: synthesis and characterization of zinc phthalocyanines bearing phenyl substituents at the 1-, 4-, 8-, 11-, 15-, 18-, 22-, and/or 25-positions. *Chem Eur J* 2005;11:5205–16.
- [38] Wang B, Li Z, Zuo X, Wu Y, Wang X, Chen Z, et al. Preparation, characterization and NO₂-sensing properties of octa-iso-pentyloxyphthalocyanine lead spin-coating films. *Sens Actuators B* 2010;149:362–7.